

2



AD-A175 110

ASSESSMENT OF DAMAGE TOLERANCE REQUIREMENTS AND ANALYSES

Volume I - Executive Summary

M. LEVY

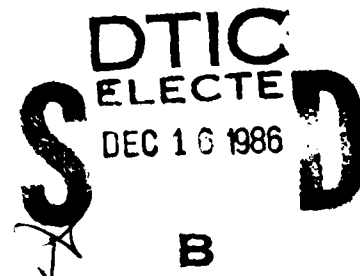
Fairchild Industries
Fairchild Republic Company
Farmingdale, N.Y. 11735

SEPTEMBER 1986

Final Technical Report for Period September 1982 - November 1985

DTIC FILE COPY

Approved for public release; distribution is unlimited



FLIGHT DYNAMICS LABORATORY
AIR FORCE WRIGHT AERONAUTICAL LABORATORIES
AIR FORCE SYSTEMS COMMAND
WRIGHT-PATTERSON AIR FORCE BASE, OHIO 45433-6553

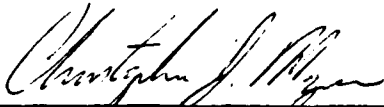
86 12 15 007

NOTICE

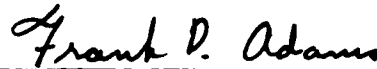
When Government drawings, specifications, or other data are used for any purpose other than in connection with a definitely related Government procurement operation, the United States Government thereby incurs no responsibility nor any obligation whatsoever; and the fact that the government may have formulated, furnished, or in any way supplied the said drawings, specifications, or other data, is not to be regarded by implication or otherwise as in any manner licensing the holder or any other person or corporation, or conveying any rights or permission to manufacture use, or sell any patented invention that may in any way be related thereto.

This report has been reviewed by the Office of Public Affairs (ASD/PA) and is releasable to the National Technical Information Service (NTIS). At NTIS, it will be available to the general public, including foreign nations.

This technical report has been reviewed and is approved for publication.



Lt Christopher J. Mazur, Project Engr
Fatigue, Fracture & Reliability Group
Structural Integrity Branch
Structures & Dynamics Division
FOR THE COMMANDER



Frank D. Adams, Acting Chief
Structural Integrity Branch
Structures & Dynamics Division



ROBERT M. BADER
Assistant Chief
Structures & Dynamics Division

If your address has changed, if you wish to be removed from our mailing list, or if the addressee is no longer employed by your organization please notify AFWAL/FAE W-PAFB, OH 45433 to help us maintain a current mailing list.

Copies of this report should not be returned unless return is required by security considerations, contractual obligations, or notice on a specific document.

REPORT DOCUMENTATION PAGE

1a. REPORT SECURITY CLASSIFICATION Unclassified		1b. RESTRICTIVE MARKING A173-110	
2a. SECURITY CLASSIFICATION AUTHORITY		3. DISTRIBUTION / AVAILABILITY OF REPORT Approved for public release; distribution unlimited.	
2b. DECLASSIFICATION / DOWNGRADING SCHEDULE			
4. PERFORMING ORGANIZATION REPORT NUMBER(S)		5. MONITORING ORGANIZATION REPORT NUMBER(S) AFWAL-TR-86-3003, Vol. I	
6a. NAME OF PERFORMING ORGANIZATION Fairchild Industries Fairchild Republic Co.	6b. OFFICE SYMBOL (If applicable)	7a. NAME OF MONITORING ORGANIZATION Flight Dynamics Laboratory (AFWAL/FIBEEC)	
6c. ADDRESS (City, State, and ZIP Code) Farmingdale, N.Y. 11735		7b. ADDRESS (City, State, and ZIP Code) Wright-Patterson Air Force Base Ohio, 45433-6553	
8a. NAME OF FUNDING / SPONSORING ORGANIZATION AFWAL	8b. OFFICE SYMBOL (If applicable) FIBEC	9. PROCUREMENT INSTRUMENT IDENTIFICATION NUMBER F33615-82-C-3215	
8c. ADDRESS (City, State, and ZIP Code) Wright-Patterson AFB OH 45433-6553		10. SOURCE OF FUNDING NUMBERS	
		PROGRAM ELEMENT NO. 62201F	TASK NO. 2401
		WORK UNIT ACCESSION NO. 01	61
11. TITLE (Include Security Classification) Assessment of Damage Tolerance Requirements and Analyses Volume I: Executive Summary			
12. PERSONAL AUTHOR(S) Meir Levy			
13a. TYPE OF REPORT Final	13b. TIME COVERED FROM Sept. 82 TO Nov. 85	14. DATE OF REPORT (Year, Month, Day) 1986 September	15. PAGE COUNT 41
16. SUPPLEMENTARY NOTATION			
17. COSATI CODES		18. SUBJECT TERMS (Continue on reverse if necessary and identify by block number)	
FIELD	GROUP	Crack Growth, Crack Initiation, Lap Joint Specimens, Stringer Reinforced Specimens, Correlations.	
13	13		
13	05		
19. ABSTRACT (Continue on reverse if necessary and identify by block number)			
<p>A structural test program of a typical aircraft structural configuration was conducted to assess the current Air Force damage tolerance design requirements defined in MIL-A-83444. The specimens, made of 2024-T3XX and 7075-T6XX, were subjected to randomized flight-by-flight spectra, representative of fighter/trainer and bomber/cargo-type loading spectra, respectively, and to constant amplitude loading spectrum. A total of 72 specimens were tested. The test results were correlated with analytical predictions using the crack growth method and combined method. As a result of this study, a recommendation is provided to the validity of MIL-A-83444, to develop guidelines for selection of critical crack locations, and to assess the state-of-the-art analytical capabilities in predicting crack growth and crack initiation time.</p> <p>This volume, Volume I of a five-volume report, presents an Executive Summary of the entire program.</p>			
20. DISTRIBUTION / AVAILABILITY OF ABSTRACT <input checked="" type="checkbox"/> UNCLASSIFIED/UNLIMITED <input type="checkbox"/> SAME AS RPT. <input type="checkbox"/> DTIC USERS		21. ABSTRACT SECURITY CLASSIFICATION UNCLASSIFIED	
22a. NAME OF RESPONSIBLE INDIVIDUAL Lt. Christopher Mazur		22b. TELEPHONE (Include Area Code) (513)255-6104	22c. OFFICE SYMBOL AFWAL/FIBEC

FOREWORD

This is Volume I of the five-volume report entitled "Assessment of Damage Tolerance Requirements and Analyses," Contract No. F33615-82-C-3215. This program has been administered by the Flight Dynamics Laboratory, Air Force Wright Aeronautical Laboratories, Air Force Systems Command, Wright Patterson Air Force Base, Ohio. James L. Rudd (AFWAL/FIBEC) was the Air Force Project Engineer through December 1985. Subsequently, Mr Rudd was replaced by Lt Christopher Mazur. Albert Kuo was FRC Program Manager and Principal Investigator through March 1985. Subsequently, Meir Levy assumed the responsibility for the completion of the program. The structural test program was performed at the University of Dayton Research Lab under the supervision of George Roth. The work associated with this program was conducted between August 1982 through May 1986 as illustrated in the Schedule attached.

The technical awareness and participation in discussions on the part of Mr Rudd and Lt Mazur, the Air Force Project Engineers, contributed to the success of the program. Special appreciation to P. Doepker from the University of Dayton for his contribution to the Structural Test Program. Special thanks to R. Kollmansberger, K. Grube and S. Saul for valuable contribution in the area of technical content of the reports. Other personnel making significant contributions were R. Eng from the Stress Department, E. Walsh from Word Processing and R. Ingenito from Graphics.

PROGRAM SCHEDULE (MAJOR TASKS)

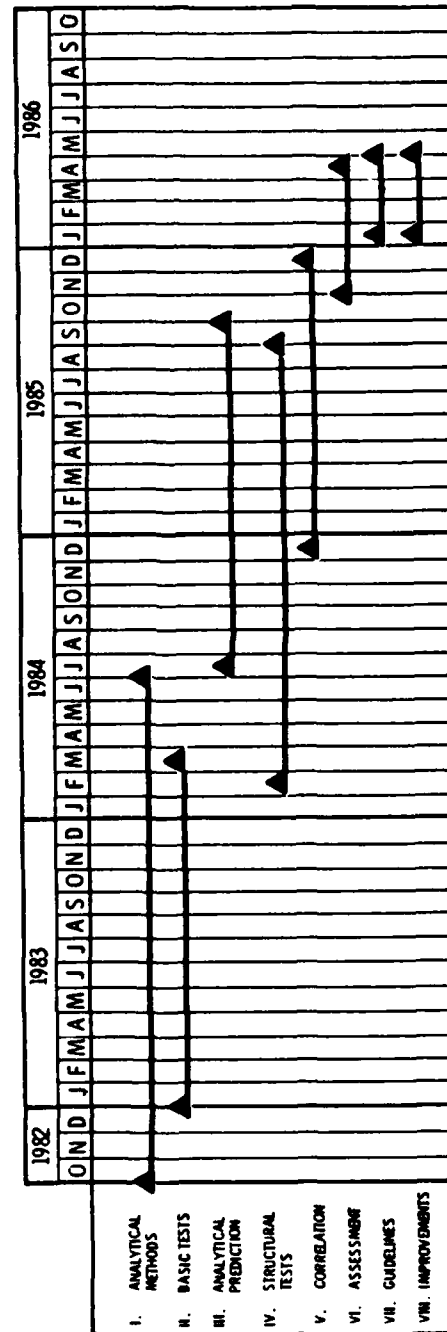


TABLE OF CONTENTS

Section	Title	Page
1.0	INTRODUCTION	1
1.1	BACKGROUND OF THE PROGRAM	2
2.0	SUMMARY OF THE PROGRAM	4
2.1	PHASE 1: SUMMARY	4
2.1.1	Analytical Methods	4
2.1.2	Governing Parameters of Fatigue Crack Initiation	4
2.1.3	Damage Accumulation	7
2.1.4	Over-Load Effect	7
2.1.5	DAMGRO Computer Program	8
2.2	BASIC TEST PROGRAM	12
2.2.1	Tensile Test Program	12
2.2.2	Crack Initiation Test Program	13
2.2.3	Fracture Toughness Test Program	17
2.2.4	Constant Amplitude Crack Growth Rates Test Program	18
2.3	PHASE 2: SUMMARY	19
2.3.1	Structural Test Program	19
2.3.2	Lap-Joint Specimens Test Program	19
2.3.3	Experimental vs. Analytical Correlations	20
2.3.3.1	Experimental Results vs. Analytical Predictions for Single-Shear Lap-Joint Specimens	21
2.3.3.2	Single-Shear Lap-Joint Specimens: Summary	23
2.3.3.3	Experimental vs. Analytical Predictions for Double-Shear Lap-Joint Specimens	23
2.3.3.4	Double-Shear Lap-Joint Specimens: Summary	25
2.3.3.5	Stringer-Reinforced Specimens Test Program	26
2.3.3.6	Experimental vs. Analytical Predictions of Stringer- Reinforced Specimen	28
2.3.3.7	Stringer-Reinforced Specimens: Summary	31
2.4	PHASE 3: SUMMARY	32
2.4.1	Task VI: Assessment of and Recommended Improvements to MIL-A-83444	32
2.4.2	Task VII: Guidelines for Most Critical Initial Primary Damage Location	32
2.4.3	Task VIII: Assessment of and Improvements to Damage Tolerance Analyses	32
2.5	RECOMMENDATIONS	32
	REFERENCES	34

DTIC
ELECTE
DEC 16 1986

B

v



DTIC TAG		<input checked="" type="checkbox"/>
Unannounced		<input type="checkbox"/>
Justification		<input type="checkbox"/>
By _____		
Distribution _____		
Availability _____		
Availability _____		
Dist	Special	
A-1		

LIST OF FIGURES

Figure	Title	Page
2.1	Crack Growth Models of Plate Sections in DAMGRO Computer Program	9
2.2	Crack Growth Models of Stringer Sections in DAMGRO Computer Program	10
2.3	Crack Initiation Models in DAMGRO Computer Program	11

LIST OF TABLES

Table	Title	Page
2.1	Average Tensile Properties	13
2.2	Summary of Crack Initiation Data for 2024-T3XX	15
2.3	Summary of Crack Initiation Data for 7075-T3XX	16
2.4	Average Fracture Toughness Properties	17
2.5	Modified Walker's Equation Coefficients	18
2.6	Lap-Joint Specimens Test Program	20
2.7	Experimental Results vs. Analytical Predictions for Single-Shear Lap-Joint Specimens Subjected to Constant Amplitude Loading Spectrum	21
2.8	Experimental Results vs. Analytical Predictions for Single-Shear Lap-Joint Specimens Subjected to A-10A Loading Spectrum	22
2.9	Experimental Results vs. Analytical Predictions for Single-Shear Lap-Joint Specimens Subjected to AMAVS Loading Spectrum	22
2.10	Experimental Results vs. Analytical Predictions for Double-Shear Lap-Joint Specimens Subjected to Constant Amplitude Loading Spectrum	24
2.11	Experimental Results vs. Analytical Predictions for Double-Shear Lap-Joint Specimens Subjected to A-10A Loading Spectrum	24
2.12	Experimental Results vs. Analytical Predictions for Double-Shear Lap-Joint Specimens Subjected to AMAVS Loading Spectrum	25
2.13	Stringer-Reinforced Specimens Test Program Matrix	27
2.14	Experimental Results vs. Analytical Predictions for Stringer-Reinforced Specimens Subjected to Constant Amplitude Loading Spectrum	28
2.15	Experimental Results vs. Analytical Predictions for Stringer-Reinforced Specimens Subjected to A-10A Loading Spectrum	29
2.16	Experimental Results vs. Analytical Predictions for Stringer-Reinforced Specimens Subjected to AMAVS Loading Spectrum	30

1.0 INTRODUCTION

Eight major tasks listed below have been planned to achieve the program objectives. These tasks encompass assessing the validity of, and recommending improvements to the current MIL-A-83444, developing guidelines for identifying the most critical initial primary damage locations for typical aircraft structures, and assessing and improving the state-of-the-art analytical methods to satisfy the requirements of MIL-A-83444.

- Task I: Analytical Methods
- Task II: Basic Tests
- Task III: Analytical Predictions
- Task IV: Structural Tests
- Task V: Analytical/Experimental Correlations
- Task VI: Assessment of and Recommended Improvements to MIL-A-83444
- Task VII: Guidelines for Selecting Most Critical Initial Primary Damage Location
- Task VIII: Assessment of and Improvements to Damage Tolerance Analyses

The material presented in this volume consists of an Executive Summary of the entire program. The other volumes issued are listed below:

- Volume II: Analytical Methods
- Volume III: Analytical Predictions and Correlations
- Volume IV: Raw Test Data
- Volume V: Assessment and Recommendations

Volume II contains the Analytical Methodology derived during Task I of the Program, including crack growth and crack initiation techniques, and results of Finite Element Modeling of stress intensity factors.

Volume III contains Analytical to Experimental Correlation of 72 Structural Test Specimens performed during Task IV of the Program.

Volume IV contains the Raw Test Data obtained during the Basic Test, and the Structural Test Programs. Requests for this document may be referred to the Flight Dynamics Laboratory (AFWAL/FIBE), Wright Patterson Air Force Base, Ohio 45433.

Volume V contains an assessment of the Damage Tolerance Design Requirements defined in MIL-A-83444, Analytical methods evaluation and a Guideline for Identifying Critical Locations for Damage Tolerance Analysis. It also contains recommendations and follow-on work.

In addition, a User Manual of the DAMGRO Computer Program has been released.

1.1 BACKGROUND OF THE PROGRAM

The recognition that failures of metallic aircraft structures are primarily caused by cracks emanating from fastener holes, and the availability of fracture mechanics methodologies to deal with cracks has led the USAF to adapt the damage tolerance approach in lieu of the safe-life approach for ensuring safety of aircraft structures. The requirements specified by the USAF to achieve a damage tolerant design are given in MIL-A-83444 (Ref. 1), which defines initial flaw assumptions, in-service inspection flaw assumptions, inspectability, and specifies residual strength requirements. However, some of the requirements are based on engineering judgment and limited data; hence they need to be updated, improved upon through analyses, and verified experimentally.

Fatigue crack growth life analysis is essential in the fulfillment of MIL-A-83444 for qualifying the service life of airframes, establishing inspection intervals, and satisfying residual strength requirements. The effectiveness of the damage tolerance approach will greatly depend on the accuracy of fatigue crack growth life analyses. To perform fatigue crack growth life analyses, assumptions must be made of specific initial primary flaw location, flaw geometry, flaw multiplicity, continuing damage, and cracking sequence for a fracture critical area. Although MIL-A-83444 gives such assumptions, it is often not detailed and specific enough for making analyses of typical structural elements without involving somewhat arbitrary assumptions. Experience has indicated that varying these assumptions often results in substantial differences in

fatigue crack growth lives. In particular, the most critical locations for initial primary damage are not obvious for the complex geometries involved in aircraft structures. Thus, guidelines are needed for identifying the most critical initial primary damage locations.

In the design analysis of airframes, the complexities of numerous structural details, assumption of the initial crack locations and flaw geometries, and possible cracking sequence have necessitated the consideration of time and cost required for the analysis. The compounded solution method is well suited for the design and has been commonly used in the aircraft industry. However, a thorough assessment of the accuracy of this relatively simple method is needed for complex aircraft structural configurations and loadings.

Current damage tolerance analysis is based on fracture mechanics which presumes the existence of initial flaws. However, it is often observed that the growth of initial primary damage is arrested at an adjacent boundary or fastener hole. In order to continue the analysis of subsequent cracking behavior, current MIL-A-83444 assumes that the initial continuing damage having specified sizes and shapes exists at specified locations. Such assumptions are necessary because fracture mechanics cannot be used to predict the reinitiation time of an arrested crack; in particular, these assumptions often result in conservative structural life predictions. One promising method of predicting the reinitiation time involves the use of baseline fatigue crack initiation data and the concept of stress severity factor. A study of this method was made in Ref. 3; however, improvement and verification of such a crack reinitiation analysis is needed to assess the initial continuing damage assumptions in MIL-A-83444 and the associated analyses.

The previously completed USAF contract F33615-75-C-3093 (Ref. 2) was directed toward resolving the above problems. The effort of that contract has resulted in recommended improvements to MIL-A-83444 and the associated analyses, and has exposed the deficiency in crack reinitiation analysis. However, the conclusions were based on a single material and constant amplitude load tests. Therefore, such conclusions must be further verified and substantiated by extensive experimental and analytical studies which use realistic aircraft structural configurations, manufacturing processes, and service stress spectra.

2.0 SUMMARY OF THE PROGRAM

This program consisted of three Phases including eight Tasks. Phase 1 consisted of Tasks I, II and III; Phase 2 consisted of Tasks IV and V; Phase 3 consisted of Tasks VI, VII and VIII.

2.1 PHASE 1: SUMMARY

The objectives of Phase 1 were to provide analytical formulation of the crack growth and crack initiation methodology, to provide basic material allowables and to perform crack growth and crack initiation predictions of the structural test specimens. Phase 1 involved three tasks: Tasks I, II and III.

2.1.1 Analytical Methods

During Task I of the program, an assessment of and improvement to the state-of-the-art analytical methods to predict crack growth and crack initiation was conducted. A major effort of Task I was focused on improving the compounded stress intensity solution of various structural configurations, and in deriving of stress severity factors to predict crack initiation. Volume II of the report presents the results of Task I efforts.

2.1.2 Governing Parameters of Fatigue Crack Initiation

Since the local concentration of plastic strain at a notch root (i.e., edge of a hole) causes fatigue crack initiation of notched structural members, an accurate prediction of fatigue crack initiation time will require the reliable characterization of stress/strain at the very edge of a notch root. The strain energy density, S , was proposed herein as the governing parameter to characterize the true peak stress/strain at a notch root. The strain energy density was derived in Volume II of the report using the stress severity factor (Ref. 4), Neuber's rule (Ref. 5), and material size effect (Ref. 6).

The stress/strain at the edge of a hole is determined not only by the fastener hole itself relative to far field stress and remote (by-pass) loads but also by the effects due to hole-fastener interference, preload in a fastener, and faying surface condition. These effects cannot be accurately determined by analysis alone. Analysis enhanced with experimental data should yield acceptable

accuracy. Therefore, the concept of stress severity factor proposed by Jarfall (Ref. 4) is selected as a suitable parameter for characterizing the elastic stress concentration at the edge of a fastener hole or internal notch subjected to both fastener and remote loads. The stress severity and elastic concentration factors are redefined in the two following equations,

$$k = \alpha \beta \gamma \cdot k_t \quad (2.1)$$

$$k_t = \frac{1}{\sigma_0} \left\{ \frac{(1-C)P}{Wt} k_{tg} + \frac{CP}{2rt} k_{tb} k_{td} \right\} \quad (2.2)$$

remote load fastener load

Where: k = stress severity factor,
 α = coefficient to account for hole fastener interference,
 β = coefficient to account for preload in a fastener,
 γ = coefficient to account for faying surface condition,
 k_t = elastic stress concentration factor for a fastener hole including both fastener load and remote load,
 σ_0 = P/Wt = effective gross section stress surface condition,
 P = total applied load,
 C = fraction of load-transfer through fastener,
 r = hole radius,
 W = plate width,
 t = plate thickness,
 k_{tb} = elastic stress concentration factor for fastener load assuming rigid fastener and no fastener tilting,
 k_{td} = elastic stress concentration factor to account for fastener tilting and fastener deflection,
 k_{tg} = elastic stress concentration factor for remote load.

An important fatigue phenomenon which needs to be considered to achieve accurate fatigue crack initiation time is the "material size effect." It is a fact that the fatigue notch factor is lower than the theoretical elastic stress concentration factor, k_t . This fact implies that the real peak notch stress experienced by the material at the notch root is lower than that calculated by the theoretical elastic stress concentration factor.

The recognition of such a necessity is evidenced by the inclusion of the Neuber's "material size effect" correction to k_t in the specification of metal fatigue data as contained in MIL-HDBK-5D (Ref. 7). Neuber proposed the following "effective stress concentration factor" to account for "material size effect":

$$k_N = 1 + \frac{(k_t - 1)}{1 + \sqrt{\rho/R}} \quad (2.3)$$

where R is the notch root radius; the parameter ρ is Neuber's material constant which is available for aluminum and steel in Refs. 8 and 9 respectively.

The strain energy density, S as defined in Equation (2.4), was adapted in this investigation to characterize the true peak stress/strain. To account for the effects of hole-fastener interference, preload in a fastener, and faying surface condition, the stress severity factor k as redefined in Equation (2.5) is used, in lieu of k_N :

$$S = \frac{1}{2} \frac{(k \sigma_o)^2}{E} \quad (2.4)$$

$$k = \text{stress severity factor} = \alpha\beta\gamma \cdot k_N \quad (2.5)$$

Experimental tests to be described later are required to provide basic fatigue crack initiation data for the analysis. The total fatigue life from testing, N , was plotted against strain energy density, S , using a log-log scale. The data was represented by a best-fit equation in the following form:

$$S_{\max} = S_f N^m \quad (2.6)$$

where S_{\max} is the maximum strain density and S_f can be interpreted as a material constant corresponding to $N = 1$.

Since there are different stress ratios in a fatigue stress spectrum, an N vs S_{\max} equation should account for stress ratio effects in a manner similar to that of da/dN vs K_{\max} for fatigue crack growth rates. This was accomplished by employing the well-known Goodman Diagram which has been used in MIL-HDBK-50 (Ref. 7) to present constant amplitude fatigue data. A linear approximation (in terms of strain energy density) was adopted to construct a constant-life diagram (Goodman Diagram).

It was shown in Volume II that the number of cycles to failure may be related to the maximum strain energy density listing Equation 2.7, where R is the stress ratio

$$N = \left(\frac{(1-R) S_{\max}}{S_f - R S_{\max}} \right)^{\frac{1}{m}} \quad (2.7)$$

2.1.3 Damage Accumulation

Equation (2.7) gives the total life as a function of constant strain energy density. However, the strain energy density is a variable for a given component subjected to a fatigue stress spectrum because it is determined by the stress severity factor which varies with crack length and gross section stress, τ_0 . Thus, to predict fatigue crack initiation under spectrum loading, cumulative damage computations must be performed. The Palmgren-Miner approach of linear cumulative damage was employed in this investigation.

2.1.4 Overload Effect

Spectrum overload is assumed to have an effect not only on crack growth life but also on crack initiation life. Thus, it needs to be considered in the analysis to achieve a realistic prediction of fatigue crack initiation time. There have been a number of theoretical models to treat overload effects in crack growth analysis, but no such models exist for crack initiation. The Willenborg model (Ref. 11), which represents one of the state-of-the-art retardation models in crack growth analysis, was employed by Brussat et al. (Ref. 10) to treat the beneficial effects due to overloads in fatigue crack initiation analysis. However, Brussat et al. did not describe how the Willenborg model was applied to fatigue crack initiation. A mathematical approach similar to the Willenborg model was employed in this investigation.

2.1.5 DAMGRO Computer Program

A computer program "DAMGRO" (Damage Growth) was developed, based upon the theories presented above. The computer program was written in FORTRAN language. In DAMGRO, the crack growth analysis is treated in a manner similar to the CRKGRO (Ref. 12) computer program except that the improved stress intensity factor solutions are incorporated into DAMGRO.

Using DAMGRO, structural life can be predicted with any one of the following three methods: namely (i) crack growth only, (ii) combined crack growth and initiation, and (iii) crack initiation only. The adequacy of methods (i) and (ii) was evaluated through correlation with experimental results. Method (iii) is similar to the traditional fatigue analysis as adopted in the safe-life approach; thus, no experimental verification of this method was performed.

The "DAMGRO" computer program contains ten subroutines to calculate stress intensity factors and six subroutines to calculate stress severity factors. The structural models corresponding to these sixteen subroutines are shown in Figures 2.1 through 2.3. These models cover many situations encountered in airframe design. The cracks in all of the models can be either through-the-thickness or corner cracks.

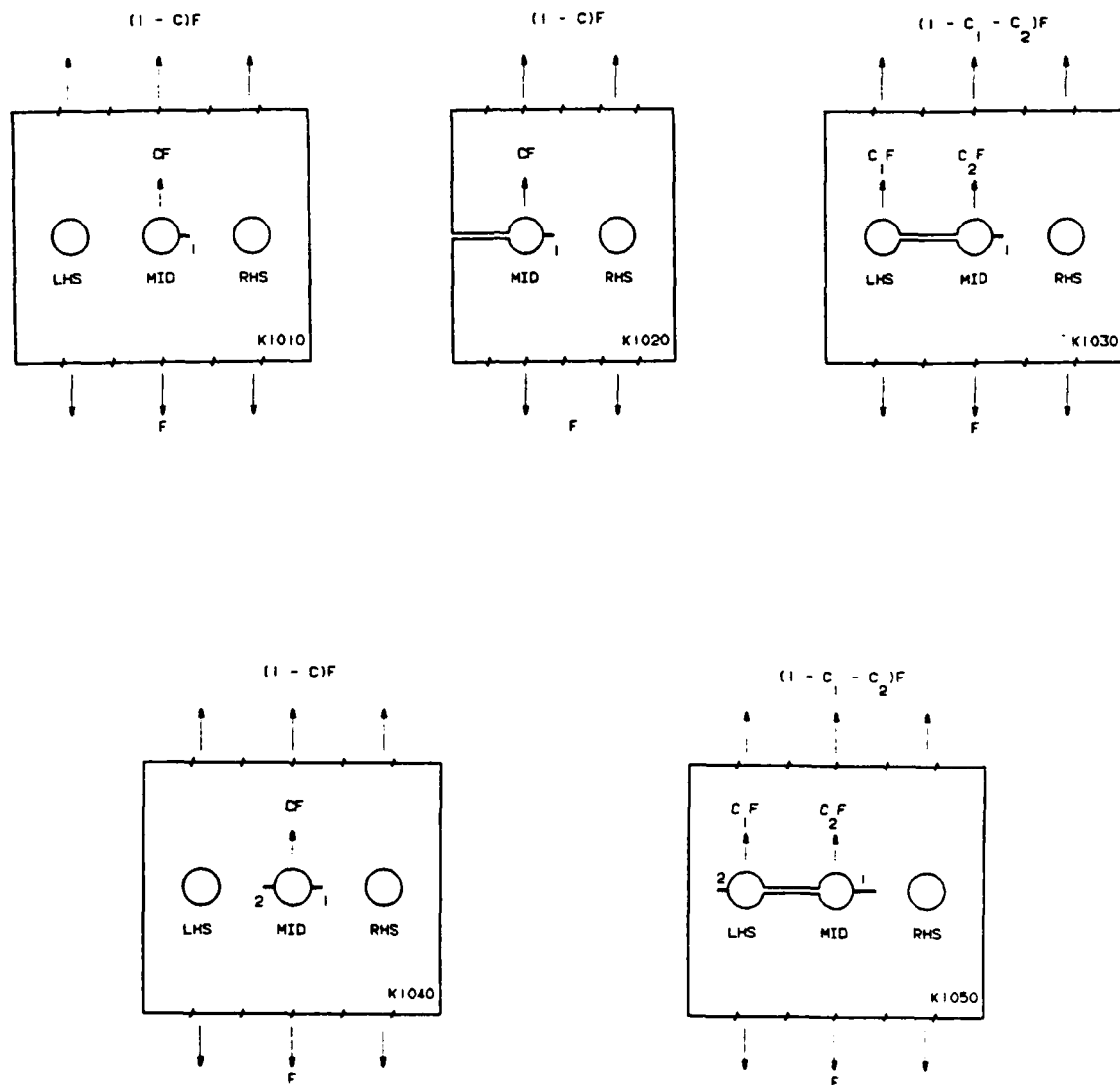
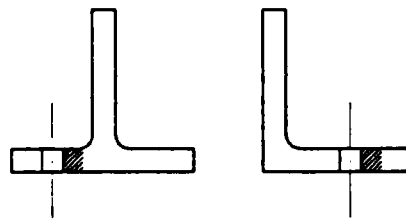
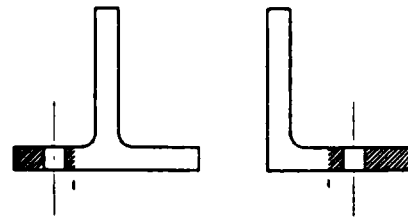


Figure 2.1. Crack Growth Models of Plate Sections in DAMGRO Computer Program

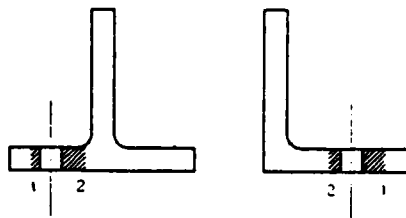
CRACK CAN BE ON
EITHER SIDE OF
THE HOLE.



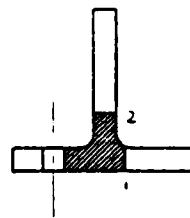
K2010



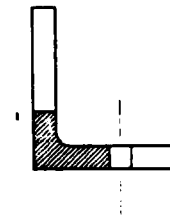
K2020



K2040



K2050



K2060

Figure 2.2. Crack Growth Models of Stringer Sections in DAMGRO
Computer Program

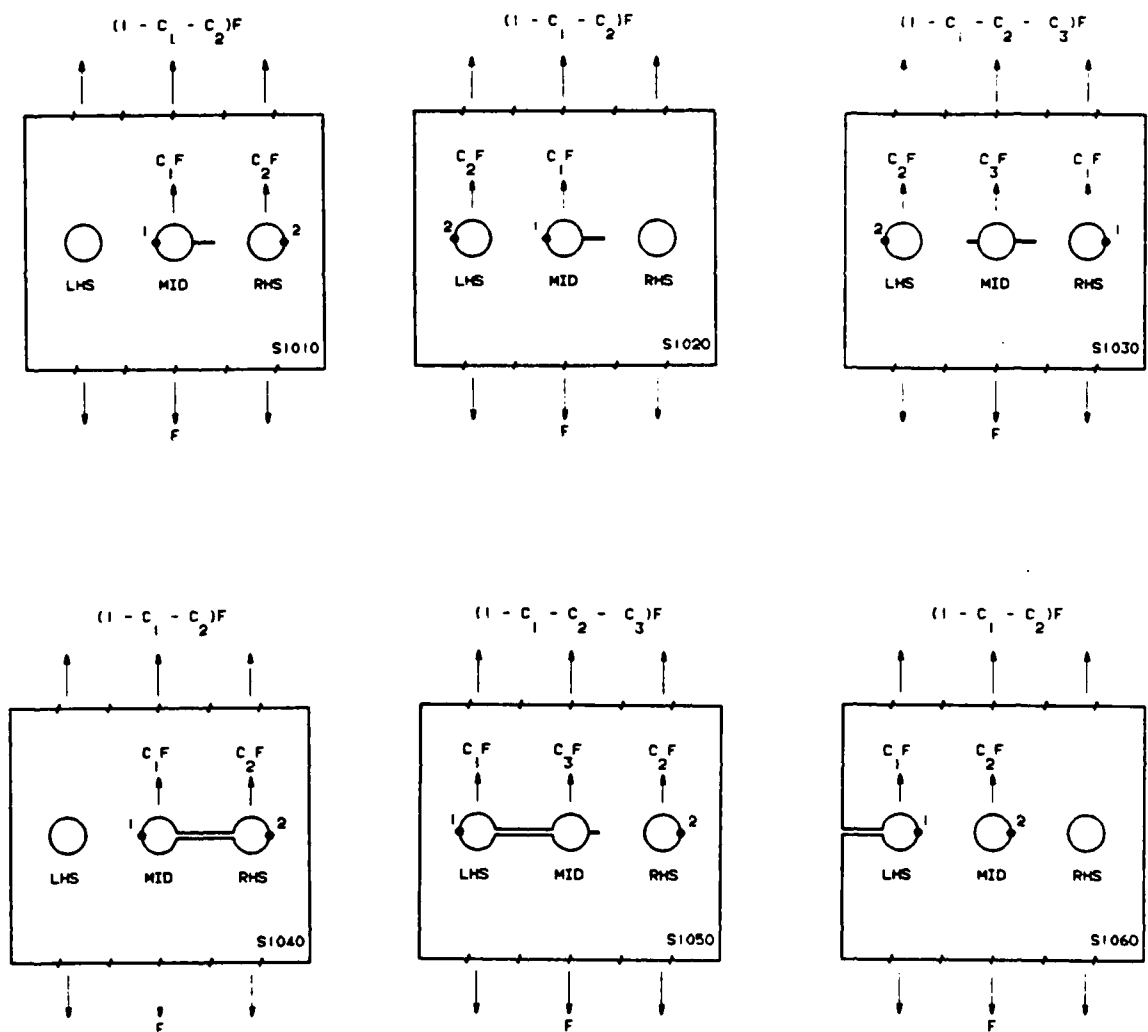


Figure 2.3. Crack Initiation Models in DAMGRO Computer Program

2.2 BASIC TEST PROGRAM

The purpose of the basic test program was to generate a crack growth and crack initiation data base for material forms similar to those used in the structural test program. A total of 224 specimens were tested. They included 60 tensile specimens, 80 crack initiation specimens, 20 fracture toughness specimens, and 64 constant amplitude crack growth specimens. The materials selected for the entire program were 2024-T3XX and 7075-T6XX.

2.2.1 Tensile Test Program

The purpose of the Tensile Test program was to evaluate the mechanical properties of material forms used during the structural test program of Task IV. Various product forms were evaluated to include, sheet, plate and extrusion sections in both longitudinal and transverse grain directions. The allowables obtained included yield strength, ultimate strength, % elongation and Young's modulus. The test results indicated that the majority of the allowables were superior to the A-Allowables given in the military standard MIL-5D. A summary of the average tensile properties obtained during the test program is given in Table 2.1.

TABLE 2.1. AVERAGE TENSILE PROPERTIES

PRODUCT FORM	YIELD STRENGTH (KSI)		ULTIMATE STRENGTH (KSI)		ELONGATION (%)		YOUNG'S MODULUS (KSI * 10 ³)	
	LONG.	TRAN.	LONG.	TRAN.	LONG.	TRAN.	LONG.	TRAN.
2024-T3 0.19" Sheet	53.1	45.0	67.4	67.2	14.8	18.0	10.7	11.0
2024-T3 0.09" Sheet	52.9	42.5	69.0	67.5	17.0	19.2	11.4	10.2
2024-T351 0.25" Plate	51.1	45.4	70.0	67.0	20.2	18.8	10.5	11.0
2024-T3511 0.19" Tee	53.3	50.5	67.4	62.6	17.8	7.5	11.0	10.7
2024-T3511 0.25" Angle	47.6	43.2	62.3	58.9	21.3	10.7	11.1	10.3
7075-T651 0.31" Plate	77.9	75.4	82.7	84.1	13.5	12.8	10.1	10.2
7075-T6 0.16" Sheet	77.2	73.8	81.6	84.3	15.0	13.3	10.4	10.8
7075-T651 0.4" Plate	77.2	72.6	79.6	79.4	13.8	11.5	11.1	10.7
7075-T6511 0.31" Tee	78.9	69.7	86.2	76.6*	12.8	9.3	10.9	10.3
7075-T6511 0.31" Angle	82.7	77.2	89.2	85.2	11.8	11.0	10.4	10.2

*Below A-allowable, i.e. 78.0

2.2.2 Crack Initiation Test Program

The purpose of the crack initiation test program was to provide fatigue initiation allowables for the product form used during the structural test program.

A total of eighty (80) crack initiation specimens were tested. The specimens were made of 2024-T3 and 7075-T6 aluminum alloys, and subjected to constant amplitude loading with various stress levels as indicated in Tables 2.2 and 2.3. Five groups were tested: (i) Baseline specimens with an open hole, (ii)

Group A specimens, with various degree of load transfer, clearance fit holes, no clamp-up and no presence of sealant at the faying surface, (iii) Group B specimens, with interference fit, no clamp-up and no presence of sealant (iv) Group C specimens with interference fit, clamp-up and no sealant, and (v) Group D specimens with interference fit, clamp-up and presence of sealant. The baseline group and Group A provided baseline coefficients for equation 2.6. The test data of Groups B, C and D were originally intended to obtain the empirical constants α , β and γ which account for the effects of interference-fit, clamp-up and sealant, respectively. However, because of the relatively small number of specimens and the scatter in life associated with them, distinction between α , β and γ could not be made. Therefore, the product $\alpha\beta\gamma$ was obtained to account for the combined effect of interference, clamp-up and sealant.

The crack growth lives N_g of all the specimens were predicted using the "DAMGRO" computer program. The initial flaw assumed for each specimen was a 0.05-inch quarter-circular corner crack. The life required to initiate a 0.05-inch quarter-circular corner crack is defined as $(N_p - N_g)$ where N_p is the total life. The damage index d_i for the initiation of a 0.05 inch quarter-circular corner crack is defined as $d_i = (N_p - N_g)/N_p$.

The calculated value of d_i were then curve-fitted into equation 2.8.

$$d_i = C_1 - C_2 S_{\max} \quad (2.8)$$

where C_1 , C_2 are the damage coefficients evaluated for 2024-T3 and 7075-T6 aluminum alloys, and for the two groups of specimens.

Note that Equation (2.8) represents the damage index for the initiation of a 0.05-inch quarter-circular corner crack for the specimens subjected to constant amplitude fatigue loading. For the case of spectrum loading, the damage index D_f to initiate an 0.05 inch quarter-circular corner crack was determined using the weighted method.

TABLE 2.2. SUMMARY OF CRACK INITIATION DATA FOR 2024-T3XX

GROUP	LOAD TRANSFER	OPEN HOLE	SPECIMEN'S CONFIGURATION				MAX. STRESS σ_o (Ksi)	MAX. STRAIN ENERGY DEN- SITY S (Ksi)	TEST LIFE TO FAILURE N_t (CYCLES)
			INTER- FERENCE	CLEAR- ANCE	CLAMP- UP	SEAL- ANT			
BASE LINE	None	Yes			No	No	34.0	0.33	11,225
	None	Yes			No	No	28.0	0.23	20,956
	None	Yes			No	No	16.0	0.28	7,872
	None	Yes			No	No	20.0	0.44	3,970
A	8.4%			Yes	No	No	18.0	0.11	Not Fail
	29.2%			Yes	No	No	32.0	0.55	8,649
	9.1%			Yes	No	No	25.0	0.79	1,451
	32.8%			Yes	No	No	20.0	0.66	3,790
B	None		Yes		No	No	34.0	0.33	84,050
	None		Yes		No	No	18.0	0.36	14,570
	24.8%		Yes		No	No	16.0	0.11	84,648
	26.7%		Yes		No	No	20.0	0.61	10,427
C	8.4%		Yes		Yes	No	34.0	0.39	19,044
	29.2%		Yes		Yes	No	24.0	0.31	71,972
	9.1%		Yes		Yes	No	22.0	0.61	30,313
	32.8%		Yes		Yes	No	20.0	0.66	20,715
D	24.8%		Yes		Yes	Yes	34.0	0.52	16,216
	24.8%		Yes		Yes	Yes	20.0	0.18	232,957
	32.8%		Yes		Yes	Yes	14.0	0.32	156,386
	32.8%		Yes		Yes	Yes	20.0	0.66	33,235

TABLE 2.3. SUMMARY OF CRACK INITIATION DATA FOR 7075-T6XX

GROUP	SPECIMEN'S CONFIGURATION						MAX. STRESS σ_o (Ksi)	MAX. STRAIN ENERGY DEN- SITY S (ksi)	TEST LIFE TO FAILURE N_t (CYCLES)
	LOAD TRANSFER	OPEN HOLE	INTER- FERENCE	CLEAR- ANCE	CLAMP- UP	SEAL- ANT			
BASE LINE	None	Yes			No	No	34.0	0.38	6,085
	None	Yes			No	No	28.0	0.26	15,225
	None	Yes			No	No	16.0	0.33	10,214
	None	Yes			No	No	20.0	0.52	2,563
A	8.4%			Yes	No	No	18.0	0.13	80,890
	29.2%			Yes	No	No	32.0	0.64	3,745
	9.1%			Yes	No	No	25.0	0.93	1,022
	32.8%			Yes	No	No	9.5	0.17	3,346
B	None		Yes		No	No	34.0	0.38	94,066
	None		Yes		No	No	18.0	0.42	91,936
	24.8%		Yes		No	No	16.0	0.13	118,926
	26.7%		Yes		No	No	20.0	0.72	6,421
C	8.4%		Yes		Yes	No	34.0	0.45	11,784
	29.2%		Yes		Yes	No	24.0	0.36	22,922
	9.1%		Yes		Yes	No	22.0	0.72	13,840
	32.8%		Yes		Yes	No	9.5	0.17	374,502
D	24.8%		Yes		Yes	Yes	34.0	0.61	7,982
	24.8%		Yes		Yes	Yes	20.0	0.21	51,427
	32.8%		Yes		Yes	Yes	14.0	0.38	25,328
	32.8%		Yes		Yes	Yes	9.5	0.17	225,088

2.2.3 Fracture Toughness Test Program

The purpose of the fracture toughness test program was to establish fracture toughness allowables for the material forms used during the structural test program. A test of 20 specimens provided material resistance curves, 'R-Curves' and critical fracture toughness allowables. The apparent fracture toughness, K_{APP} , given in Equation (2.9) and the critical fracture toughness, K_{IC} , Equation (2.10) were also determined.

$$K_{APP} = \frac{P_{max}}{Wt} \sqrt{\pi a_o \sec \frac{\pi a_o}{W}} \quad (2.9)$$

$$K_{IC} = \frac{P_{max}}{Wt} \sqrt{\pi a_f \sec \frac{\pi a_f}{W}} \quad (2.10)$$

Where a_o , a_f are the initial and the final half crack length respectively, P_{max} is the failure load, and W and t are the specimens width and thickness respectively. A summary of the average fracture toughness allowables are provided in Table 2.4.

TABLE 2.4. AVERAGE FRACTURE TOUGHNESS PROPERTIES

MATERIAL FORM	NUMBER OF SPECIMENS	THICKNESS (IN)	WIDTH (IN)	K_{app} (Ksi \sqrt{in})	K_{IC} (Ksi \sqrt{in})
2024-T3 Sheet	2	0.193	12.0	83.00	116.00
2025-T3 Sheet	2	0.088	18.0	98.95	155.90
2024-T351 Plate	2	0.253	8.0	75.92	100.00
2024-T3511 Ext. (TEE)	2	0.188	2.75	43.88	58.00
2024-T3511 Ext. (ANGLE)	2	0.238	2.25	43.85	62.40
7075-T651 Plate	2	0.324	3.0	47.37	61.34
7075-T651 Plate	2	0.406	3.0	41.07	53.45
7075-T6 Sheet	2	0.157	12.0	82.25	97.62
7075-T6511 Ext. (TEE)	2	0.300	2.75	55.68	77.56
7075-T6511 Ext. (ANGLE)	2	0.310	2.75	51.72	67.33

2.2.4 Constant Amplitude Crack Growth Rate Test Program

The purpose of the constant amplitude crack growth rate test program was to establish a crack growth rate data base for the material form used during the structural test program. The test data were fitted into the "Modified Walker Equation" in term of da/dN vs K_{max} given in Equation (2.11).

$$\frac{da}{dN} = c \left((1 - R)^m K_{max} \right)^n \quad (2.11)$$

Where c , m and n are constant evaluated from test data, K_{max} is the maximum stress intensity factor, R is the stress ratio.

A total of 64 specimens were tested. The stress ratios tested were -0.30, -0.05, +0.05 and +0.50. The test specimens provided sufficient data for the creation of two (2) sets of the Walker's Equation constants. One for $R \geq 0$ and the second for $R < 0$. The Walker's constants are summarized in Table 2.5.

TABLE 2.5. MODIFIED WALKER'S EQUATION COEFFICIENTS

PRODUCT FORM	NUMBER OF SPECIMENS	STRESS RATIO	c	m	n
2024-T Sheet	4	positive	2.2374E-09	0.70	3.3386
2024-T3 Sheet	4	negative	6.2126E-09	0.00	2.9783
2024-T351 Plate	4	positive	7.7269E-09	0.65	2.8180
2024-T351 Plate	4	negative	4.5865E-8	0.00	2.2338
2024-T3511 Angle	4	positive	7.6198E-11	0.60	4.5667
2024-T3511 Angle	4	negative	4.3322E-11	1.00	4.0093
2024-T3511 Tee	4	positive	1.5998E-10	0.65	4.5545
2024-T3511 Tee	4	negative	2.3033E-09	1.00	3.1154
7075-T6 Sheet	4	positive	1.3579E-07	0.50	1.9752
7075-T6 Sheet	4	negative	1.0654E-07	0.00	2.0950
7075-T651 Plate	4	positive	1.7000E-08	0.50	2.8033
7075-T651 Plate	4	negative	2.6409E-08	0.00	2.4962
7075-T6511 Angle	4	positive	1.9047E-08	0.50	2.6640
7075-T6511 Angle	4	negative	3.1758E-08	0.00	2.5814
7075-T6511 Tee	4	positive	9.7285E-08	0.55	2.0369
7075-T6511 Tee	4	negative	5.8669E-08	0.00	2.4602

2.3 PHASE 2: SUMMARY

During Phase 2 of the program, two tasks were completed, Task IV and Task V. Task IV consisted of the manufacturing and testing of structural test specimens including lap-joint specimens, and stringer-reinforced specimens. Task V consisted of crack growth correlations of the experimental results vs. the analytical predictions. The purpose of the correlations was to evaluate the effectiveness of the analytical methods used to predict crack growth and crack initiation of structural elements representative of those used in airframe structure.

2.3.1 Structural Test Program

Task IV consisted of the manufacturing and testing of 72 structural test specimens. They included 36 lap-joint specimens, and 36 stringer-reinforced specimens. The material used was 2024-T3XX and 7075-T6XX aluminum alloys. The specimens were subjected to a constant amplitude loading and to randomized flight-by-flight loading spectra. The testing was performed using a MTS Hydraulic computer-controlled testing machine with loading frequency not exceeding 10Hz. The tests were conducted at Lab-Air environment. The specimens were precracked prior to assembly. The precracking was done by means of saw-cut, followed by the application of constant amplitude loading until the desired initial 0.050-inch corner flaw as achieved. During the test, crack measurements were taken using a magnifying glass. Following the test, fractographic examination was conducted on representative specimens.

2.3.2 Lap-Joint Specimen Test Program

Thirty-six lap-joint specimens were tested. It included two configurations. Eighteen specimens had a single-shear configuration, and eighteen had a double-shear configuration. Three groups of specimens were tested. They included the following:

- (a) Group A, base line with clearance fit hole, no clamp-up, and no sealant at faying surface.
- (b) Group C, with interference fit Hi-Loks, clamp-up, and no sealant present
- (c) Group D, with interference fit, clamp-up and sealant at faying surface.

The test matrix is presented in Table 2.6.

TABLE 2.6. LAP-JOINT SPECIMENS TEST PROGRAM

GROUP	CONFIGURATION	SPECIMEN INTER- FER.	CONFIGURATION CLAMP- UP	SEALANT	NUMBER OF SPECIMENS	APPLIED SPECTRUM	MAXIMUM STRESS (KSI)
A	Single-Shear	No	No	No	2	C.A.(1)	17.0
		No	No	No	2	A-10A	37.75
		No	No	No	2	AMAVS	37.75
C	Single-Shear	Yes	Yes	No	2	C.A.(1)	17.0
		Yes	Yes	No	2	A-10A	37.75
		Yes	Yes	No	2	AMAVS	37.75
D	Single-Shear	Yes	Yes	Yes	2	C.A.(1)	17.0
		Yes	Yes	Yes	2	A-10A	37.75
		Yes	Yes	Yes	2	AMAVS	37.75
A	Double-Shear	No	No	No	2	C.A.(1)	17.0
		No	No	No	2	A-10A	37.75
		No	No	No	2	AMAVS	37.75
C	Double-Shear	Yes	Yes	No	2	C.A.(1)	13.1
		Yes	Yes	No	2	A-10A	37.75
		Yes	Yes	No	2	AMAVS	37.75
D	Double-Shear	Yes	Yes	Yes	1	C.A.(2)	13.1
		Yes	Yes	Yes	3	A-10A	37.75
		Yes	Yes	Yes	2	AMAVS	37.75

(1) Stress ratio $R = 0.36$ (2) Stress ratio $R = 0.10$

2.3.3 Experimental vs. Analytical Correlations

During Task V of the program, correlations in crack growth rates of the experimental results vs. analytical predictions were performed. The correlations included 36 lap-joint specimens and 36 stringer-reinforced specimens. The purpose of the correlations was to evaluate the effectiveness of the analytical methods in predicting the crack growth lives of structural specimens subjected to a loading spectrum.

2.3.3.1 Experimental Results vs. Analytical Predictions for Single-Shear Lap-Joint Specimens

The experimental vs. analytical crack growth predictions for the single-shear lap-joint specimens subjected to constant amplitude loading spectrum are summarized in Table 2.7. Fractographic examination of the specimens subsequent to failure indicate crack initiation at the edge of most of the holes. Method 2 predicts initiation at the opposite side of the hole from where the initial flaw existed. However, Method 2 overall accuracy is about the same as Method 1. The prediction of crack initiation resulted in better indication of the presence of cracking within the fracture surface.

TABLE 2.7. EXPERIMENTAL RESULTS VS. ANALYTICAL PREDICTIONS FOR SINGLE-SHEAR LAP-JOINT SPECIMENS SUBJECTED TO CONSTANT AMPLITUDE LOADING SPECTRUM

GROUP (REF. TABLE 2.16)	MAXIMUM* STRESS (KSI)	AVERAGE TEST RESULTS TO FAILURE (CYCLES)	ANALYTICAL PREDICTIONS			
			METHOD 1		METHOD 2	
			LIFE (CYCLES)	% DEV	LIFE (CYCLES)	% DEV
A	17.0	45,250	40,730	9.9	30,555	32.5
C	17.0	96,700	40,730	46.2	67,724	30.0
D	17.0	79,105	40,730	49.2	41,289	41.8
EXPERIMENTAL/ANALYTICAL OVERALL DEV				35.1		34.7

*R=0.36

The experimental and analytical crack growth predictions for the single-shear lap-joint specimens subjected to A-10A loading spectrum are presented in Table 2.8. Overall predictions of Method 2 is more accurate than Method 1 predictions. This was primarily due to better prediction of Group C specimens. The majority of the specimens exhibited crack initiation at the edge of most of the holes, although the bulk of the growth occurred primarily at the initially flawed hole.

TABLE 2.8. EXPERIMENTAL RESULTS VS. ANALYTICAL PREDICTIONS FOR SINGLE-SHEAR LAP-JOINT SPECIMENS SUBJECTED TO A-10A LOADING SPECTRUM

GROUP (REF. TABLE 2.16)	MAXIMUM STRESS (KSI)	AVERAGE TEST RESULTS TO FAILURE (CYCLES)	ANALYTICAL PREDICTIONS			
			METHOD 1		METHOD 2	
			LIFE (CYCLES)	% DEV	LIFE (CYCLES)	% DEV
A	37.75	44,594	24,408	45.2	15,087	66.2
C	37.75	59,798	24,408	59.18	53,138	11.1
D	37.75	41,365	24,408	40.1	20,473	50.5
EXPERIMENTAL/ANALYTICAL OVERALL DEV				48.2		42.6

The experimental and analytical crack growth predictions for the single-shear lap-joint specimens subjected to AMAVS loading spectrum are presented in Table 2.9. The overall predictions using both Method 1 and Method 2, were in the un-conservative side. Both Method 1 and Method 2 predicted longer lives than the experimental results indicated.

TABLE 2.9. EXPERIMENTAL RESULTS VS. ANALYTICAL PREDICTIONS FOR SINGLE-SHEAR LAP-JOINT SPECIMENS SUBJECTED TO AMAVS LOADING SPECTRUM

GROUP (REF. TABLE 2.16)	MAXIMUM STRESS (KSI)	AVERAGE TEST RESULTS TO FAILURE (CYCLES)	ANALYTICAL PREDICTIONS			
			METHOD 1		METHOD 2	
			LIFE (CYCLES)	% DEV	LIFE (CYCLES)	% DEV
A	37.75	5,387	22,189	-310.0	9,132	- 69.5
C	37.75	11,105	22,189	- 99.8	23,343	-110.0
D	37.75	9,980	22,189	-125.0	9,944	0.0
EXPERIMENTAL/ANALYTICAL OVERALL DEV				-178.3		- 59.8

2.3.3.2 Single-Shear Lap-Joint Specimens: Summary

The following observations were concluded from the experimental and the analytical results of the single-shear lap-joint specimens.

(i) Experimental Results

- o The highest number of cycles to failure were obtained from Group C specimens. Overall, they were 85% higher than Group A and 23% higher than Group D.
- o A 23% reduction in the life of group D over Group C is attributed to the presence of sealant at the faying surface.
- o Very little crack initiation occurred in the 7075-T6XX specimens. The short life to failure may be attributed to the lack of crack initiation.

(ii) Analytical Predictions

- o In Method 1 "Crack Growth Only" the secondary damage of 0.005 in. at adjacent holes is adequate for the 2024-T3XX specimens but overly conservative for the 7075-T6XX specimens.
- o Method 2 "Crack Growth and Crack Initiation" predicted accurate crack initiation diagonally opposite the initial flaw, but did not predict initiation at adjacent holes. This is contrary to most of the experimental reports.
- o Neither method predicted accurate lives of specimens made of 7075-T6XX and both were on the unconservative side.

2.3.3.3 Experimental vs. Analytical Predictions For Double-Shear Lap-Joint Specimens

The experimental results vs. the analytical crack growth predictions for the double-shear lap-joint specimens are summarized in Table 2.10. The analytical predictions for both Method 1 and Method 2 are conservative. The overall standard deviations were about the same for both methods. However, for Group C, the predicted life using Method 2 was much closer to the test results. In all cases, Method 2 predicted crack initiation diagonally opposite the initial flaw. This was consistent with the test results.

TABLE 2.10. EXPERIMENTAL RESULTS VS. ANALYTICAL PREDICTIONS FOR DOUBLE-SHEAR LAP-JOINT SPECIMENS SUBJECTED TO CONSTANT AMPLITUDE LOADING SPECTRUM

GROUP (REF. TABLE 2.16)	MAXIMUM STRESS (Ksi)	AVERAGE TEST RESULTS	ANALYTICAL PREDICTIONS			
			METHOD 1		METHOD 2	
			LIFE (CYCLES)	% DEV	LIFE (CYCLES)	% DEV
A	13.1 R = 0.36	214,050	121,100	43.4	115,500	46.0
C	13.1 R = 0.36	2x10 ⁶	121,100	N/A	1.23x10 ⁶	N/A
D	17.0 R = 0.10	129,300	20,840	83.9	25,514	80.3
EXPERIMENTAL/ANALYTICAL OVERALL DEVIATION				63.6		63.1

The correlations for the double-shear lap-joint specimens subjected to A-10A loading spectrum are presented in Table 2.11. The standard deviation for Method 1 was 56.8% vs. 44.6% for Method 2. The better accuracy of Method 2 is attributed to Group C where Method 2 predicted closer results than Method 1.

TABLE 2.11. EXPERIMENTAL RESULTS VS. ANALYTICAL PREDICTIONS FOR DOUBLE-SHEAR LAP-JOINT SPECIMENS SUBJECTED TO A-10A LOADING SPECTRUM

GROUP (REF. TABLE 2.16)	MAXIMUM STRESS (KSI)	AVERAGE TEST RESULTS TO FAILURE (CYCLES)	ANALYTICAL PREDICTIONS			
			METHOD 1		METHOD 2	
			LIFE (CYCLES)	% DEV	LIFE (CYCLES)	% DEV
A	37.75	39,185	31,890	18.6	22,466	42.7
C	37.75	175,485	31,890	81.8	141,196	19.5
D	37.75	107,038	31,890	70.2	30,208	71.7
EXPERIMENTAL/ANALYTICAL OVERALL DEVIATION				56.8		44.6

The correlations for the double-shear lap-joint specimens subjected to an AMAVS loading spectrum are presented in Table 2.12. Again, Method 2 predictions for Group C are more accurate than Method 1 predictions. This is attributed to faying surface stress reduction used when Method 2 is utilized. The overall standard deviation is 62.8% for Method 1 vs. 58.9% for Method 2.

TABLE 2.12. EXPERIMENTAL RESULTS VS. ANALYTICAL PREDICTIONS FOR DOUBLE-SHEAR LAP-JOINT SPECIMENS SUBJECTED TO AMAVS LOADING SPECTRUM

GROUP (REF. TABLE 2.16)	MAXIMUM STRESS (KSI)	AVERAGE TEST RESULTS TO FAILURE (CYCLES)	ANALYTICAL PREDICTIONS			
			METHOD 1		METHOD 2	
			LIFE (CYCLES)	% DEV	LIFE (CYCLES)	% DEV
A	37.75	46,750	30,660	34.4	20,007	57.2
C	37.75	148,917	30,660	79.4	78,014	47.6
D	37.75	120,700	30,660	74.6	33,834	71.9
EXPERIMENTAL/ANALYTICAL OVERALL DEVIATION				62.8		58.9

2.3.3.4 Double-Shear Lap-Joint Specimens: Summary

The following observations were concluded from the experimental and the analytical results for the double-shear lap-joint specimens.

(i) Experimental Results

- o The highest number of cycles to failure was obtained from Group C specimens, by a factor of approximately 400% compared to Group A and by 44% compared to Group D.
- o Reduction in life by 44% in Group D with respect to Group C was attributed to the presence of sealant at the faying surface.
- o Crack growth is approximately the same for both upper and lower splice plates. The growth was concentrated about the initial flaw location. Little initiation occurred at adjacent fasteners.

(ii) Analytical Predictions

- o Both Methods 1 and Method 2 predictions are on the conservative side. Method 2 has overall superior predictions than Method 1. Initiation diagonally opposite the initial flaw is accurately predicted by Method 2.

2.3.3.5 Stringer-Reinforced Specimens Test Program

A total of 36 stringer-reinforced specimens were tested. This included three skin to stringer configurations, as follows:



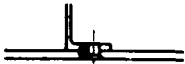
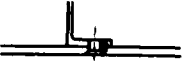

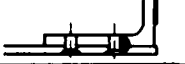





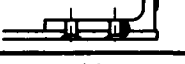






- (a) Center-stringer reinforced, continuous skin
- (b) Center-stringer reinforced, split skin
- (c) Edge-stringer reinforced, continuous skin

The specimens were made of 2024-T3XX and 7075-T6XX Aluminum Alloys. Each specimen tested had a precracked initial corner flaw of 0.050-inch located at the faying surface and common to the stringer and skin. Two locations of initial flaws were selected. One location was facing toward the upstanding leg of the stringer (inside crack), and the second, growing toward the free edge of the stringer (outside crack). An untorqued clearance-fit fastener was inserted in the precracked hole. The remaining fasteners were interference fit and fully torqued.

The specimens were subjected to a constant amplitude loading (C.A.) and to randomized loading spectrum including the A-10A and the AMAVS flight-by-flight spectra. Each of the test configurations included two duplicated tests at identical loading spectrum and initial flaw configuration.

The test matrix is shown in Table 2.13.

TABLE 2.13. STRINGER-REINFORCED SPECIMENS TEST PROGRAM MATRIX

SPECIMEN TYPE	INITIAL FLAW CONFIGURATION	INITIAL FLAW TYPE	APPLIED LOADING SPECTRUM	MAXIMUM STRESS LEVEL (ksi)	MINIMUM STRESS LEVEL (ksi)
Center T-Stringer Continuous Skin		Inside	Constant Amplt.	17.0	1.7
		Outside	Constant Amplt.	17.0	1.7
Center L-Stringer Continuous Skin		Inside	Constant Amplt.	17.0	1.7
		Outside	Constant Amplt.	17.0	1.7/4.54
Edge L-Stringer Continuous Skin		Outside	Constant Amplt.	17.0	1.7
		Inside	Constant Amplt.	17.0	1.7
Center T-Stringer Continuous Skin		Inside	AMAVS	30.5	-6.64
		Outside	AMAVS	30.5	-6.64
Center T-Stringer Split Skin		Inside	AMAVS	30.35	-6.60
		Outside	AMAVS	30.35	-6.60
Edge L-Stringer Continuous Skin		Outside	AMAVS	21.48	-4.67
		Inside	AMAVS	21.48	-4.67
Center T-Stringer Continuous Skin		Inside	A-10A	35.75	-8.34
		Outside	A-10A	35.75	-8.34
Center L-Stringer Continuous Skin		Inside	A-10A	28.0	-6.73
		Outside	A-10A	28.0	-6.73
Edge L-Stringer Continuous Skin		Outside	A-10A	35.75	-8.34
		Inside	A-10A	35.75	-8.34

2.3.3.6 Experimental Results vs. Analytical Predictions for Stringer-Reinforced Specimens

The experimental results vs. the analytical predictions for the stringer-reinforced specimens subjected to constant amplitude loading are presented in Table 2.14. The predicted lives using Method 1 and Method 2 were close to experimental results, and were conservative. Method 2 predicted crack initiation diagonally opposite the initial flaw, which was similar to the experimental results.

TABLE 2.14. EXPERIMENTAL RESULTS VS. ANALYTICAL PREDICTIONS FOR STRINGER-REINFORCED SPECIMENS SUBJECTED TO CONSTANT AMPLITUDE LOADING SPECTRUM

SPECIMEN TYPE	CRACK ORIENT- TATION	MAXIMUM GROSS STRESS (ksi)	EXPERI- MENTAL LIFE TO FAILURE (CYCLES)	ANALYTICAL PREDICTION			
				METHOD 1		METHOD 2	
				LIFE (CYCLES)	%DEV	LIFE (CYCLES)	%DEV
Center T-Stringer Continuous Skin	Inside	17.0	65,820	56,198	14.6	59,629	9.6
	Outside	17.0	65,142	57,894	11.1	48,632	25.3
Center L-Stringer Continuous Skin	Inside	17.0	76,025	64,021	15.8	60,881	19.9
	Outside	17.0	72,900	64,021	12.2	60,881	16.5
Edge L-Stringer Continuous Skin	Outside	17.0	67,136	59,579	11.3	51,158	23.8
	Inside	17.0	87,647	36,812	58.0	38,806	55.7
EXPERIMENTAL/ANALYTICAL OVERALL DEV.					20.3		25.13

The correlation for the stringer reinforced specimens subjected to A-10A loading spectrum are presented in Table 2.15. The overall standard deviation was 36.48% and 45.25% for Method 1 and Method 2, respectively. The accuracy of predictions were about the same order of magnitude except for the edge L-stringer with outside flaw, which had better prediction using Method 1.

TABLE 2.15. EXPERIMENTAL RESULTS VS. ANALYTICAL PREDICTIONS FOR STRINGER-REINFORCED SPECIMENS SUBJECTED TO A-10A LOADING SPECTRUM

SPECIMEN TYPE	CRACK ORIENT- TATION	MAXIMUM GROSS STRESS (ksi)	EXPERI- MENTAL LIFE TO FAILURE (CYCLES)	ANALYTICAL PREDICTION			
				METHOD 1		METHOD 2	
				LIFE (CYCLES)	%DEV	LIFE (CYCLES)	%DEV
Center T-Stringer Continuous Skin	Inside	35.75	191,290	111,954	41.4	103,871	45.7
	Outside	35.75	202,143	127,195	37.1	104,000	48.6
Center L-Stringer Continuous Skin	Inside	35.75	240,210	144,182	40.0	119,452	50.3
	Outside	28.0	574,875	341,174	40.6	297,818	48.2
Edge L-Stringer Continuous Skin	Outside	35.75	130,860	119,372	8.8	94,235	28.0
	Inside	35.75	151,970	74,447	51.0	74,885	50.7
EXPERIMENTAL/ANALYTICAL OVERALL DEV.					36.48		45.25

The correlation for the specimens subjected to AMAVS loading spectrum are presented in Table 2.16. The overall standard deviation was 39.83% and 47.86% for Method 1 and Method 2, respectively. Except for the specimen with the edge L-stringer outside flaw, all the predicted results were conservative.

TABLE 2.16. EXPERIMENTAL RESULTS VS. ANALYTICAL PREDICTIONS FOR STRINGER-REINFORCED SPECIMENS SUBJECTED TO AMAVS LOADING SPECTRUM

SPECIMEN TYPE	CRACK ORIENT- TATION	MAXIMUM GROSS STRESS (ksi)	EXPERI- MENTAL LIFE TO FAILURE (CYCLES)	ANALYTICAL PREDICTION			
				METHOD 1 LIFE (CYCLES)	%DEV	METHOD 2 LIFE (CYCLES)	%DEV
Center T-Stringer Continuous Skin	Inside	30.0	146,742	128,230	12.6	86,214	41.2
	Outside	30.0	180,150	107,752	40.2	95,800	46.8
Center T-Stringer Split Skin	Inside	30.0	180,269	53,865	70.1	61,476	65.9
	Outside	30.0	164,362	89,960	45.3	75,061	54.3
Edge L-Stringer Continuous Skin	Outside	20.0	259,786	281,125	-8.2	309,229	-19.0
	Inside	20.0	535,153	200,268	62.6	213,812	60.0
EXPERIMENTAL/ANALYTICAL OVERALL DEV.					39.83		47.86

2.3.3.7 Stringer-Reinforced Specimens: Summary

The following observations were concluded from the experimental and the analytical predictions of the stringer reinforced specimens.

(i) Experimental Results

- o No substantial difference in life between initial induced "inside crack" and "outside crack" for the center 'T' and center 'L' continuous skin was observed.
- o The split skin specimens indicate slightly (9.6%) shorter life for specimens with outside initial cracks then those with inside initial cracks.
- o The specimens with the edge 'L' configurations clearly indicate that the outside initial flaw contains the shorter life.
- o The split skin specimens survived 5.4% longer than the continuous skin.
- o Initiation at the opposite side of hole occurred prior to failure.
- o In most of the cases, stringers and skin failure occurred simultaneously.
- o No crack initiation was observed in split skin adjacent plate.

(ii) Analytical Predictions

- o Overall predictions were superior using Method 1 over Method 2 by approximately 20%.
- o Method 2 prediction of initiation are closer to actual test results than the assumed secondary flaw.
- o Method 2 accuracy may be improved substantially by better input parameters.
- o Both methods predict shorter lives for L-edge type specimens with outboard cracks. This is in contrary with test results.
- o The analytical methods critical crack length is much shorter than test results.

2.4 PHASE 3: SUMMARY

During Phase 3 of the contract, assessments, improvements, and recommendations were made as to the validity of the military specification MIL-A-83444, the state-of-the-art in predicting crack growth and the critical location of the initial assumed flaws. The work associated with this Phase is presented in Volume V of the Report. Phase 3 consisted of three tasks:

2.4.1 Task VI: Assessment of and Recommended Improvements to MIL-A-83444

During Task IV, assessment of the military specification MIL-A-83444 for damage tolerance design was examined. Based on the structural test program, continuing damage assumption, including size and location, was determined.

2.4.2 Task VII: Guidelines for Most Critical Initial Primary Damage Location

During Task VII, examination of the structural test specimens was performed to determine the most critical primary flaw location. Based on these data, recommendation and guidelines are made as to the location of initial primary flaws.

2.4.3 Task VIII: Assessment of and Improvements to Damage Tolerance Analyses

During Task VIII, examination of the analytical predictions of the structural test specimens were made. The validity and accuracy of 'Method 1' crack growth only, and 'Method 2' combined crack growth and crack initiation, were determined.

2.5 RECOMMENDATIONS

Based upon the results of this study, the following recommendations are offered:

- 1) Continuing damage defined in MIL-A-83444 should be revised to reflect secondary crack initiation occurring diametrically opposite the primary flaw location. The exact time of introducing the secondary flaw may depend upon the structural configuration and the stress environment. However, it is safe to assume a secondary corner flaw of 0.005-in. when the primary flaw approaches '2D' from the centerline of the hole.
- 2) An aspect ratio of 0.5 - 0.75 for corner flaws at the edge of a hole at the time the crack breaks through the thickness is more realistic than the current required by MIL-A-83444 of 1.0.

- 3) Constant amplitude crack growth rates for aluminum alloys should be developed at low stress intensity factor of 3 - 5 Ksi $\sqrt{\text{in.}}$, or at crack growth rates of 10^{-8} in/cycles. This will avoid the need of crack growth rates extrapolation.
- 4) For the majority of structural configurations, the 'outside' initial flaw is more critical than the 'inside initial flaw'. However, local geometries should be carefully evaluated prior to initial flaw selection.
- 5) The combined method analysis is a powerful tool in determining crack initiation sites. However, empirical and analytical data for crack initiation should be investigated further.
- 6) Interference fit fasteners offer the best degree of life enhancement for structure subjected to flight loads and ought to be used whenever possible.
- 7) Single-shear lap-joint configuration should be avoided whenever it is possible. Double-shear lap-joint configuration is far superior.
- 8) The presence of sealant at the faying surface tends to decrease the crack growth life, and should be treated accordingly.
- 9) Marker band cycles are a useful tool in constructing crack growth curves subsequent to failure of a test specimen. However, identification of specific sequences with time is difficult. An alternative way would be the use of a variable band repeat application, in which the number of cycles in each application is distinctly different, while maintaining the general characteristics of the "markers."

REFERENCES

1. Anon., "Airplane Damage Tolerance Requirements," MIL-A-83444 (USAF), Aeronautical Systems Division, United States Air Force, July 1974.
2. Brussat, T.R., Chiu, S.T., and Creager, M., "Flaw Growth in Complex Structure - Technical Discussion," Technical Report AFFDL-TR-77-79, Volumes 1, 2 and 3, Air Force Flight Dynamics Laboratory, December 1977.
3. Rooke, D.P. and Tweed, J., "Open-Mode Stress Intensity Factors For Two Unequal Cracks At A Hole," Royal Aircraft Establishment Technical Report, RAE TR79105, Farnborough, Hants, Britain, August 1979.
4. Jarfall, L.E., "Optimum Design of Joint, The Stress Severity Factor," Fifth ICAF Symposium, Melbourne, Australia, May 1967, pp. 49-63.
5. Neuber, H., "Theory of Stress Concentration for Shear Strained Prismatical Bodies with Arbitrary Non-Linear Stress-Strain Law," J. Appl. Mech., Dec. 1961, pp. 544-550.
6. Neuber, H., Theory of Notch Stresses: Principles for Exact Stress Calculation, J.W. Edwards (Ann Arbor, Mich), 1946: (Kerebspannungslehre: Grundlagen fur genaue Spannungsrechnung, Julius Springer (Berlin)), 1937.
7. Anon., Military Standardization Handbook: Metallic Materials and Elements for Aerospace Vehicle Structures, MIL-HDBK-5D, June 1983.
8. Kuhn, P. and Figge, I.E., "Unified Notch-Strength Analysis for Wrought Aluminum Alloys," NASA TND-1259, National Aeronautics and Space Administration, May 1962.
9. Kuhn, P. and Hardrath, H.F., "An Engineering Method for Estimating Notch-Size Effect in Fatigue Tests on Steel," NACA TN 2805, National Advisory Committee for Aeronautics, 1952.

10. Prussat, T.R., "Secondary Cracking Near A Growing Fatigue Crack," *Fatigue of Engrg. Mat. and Stru.*, Vol. 6, No. 3, 1983, pp. 281-292.
11. Willenborg, J. Engle, R.M. and Wood, H.A., "A Crack Growth Retardation Model," Technical Memorandum AFFDL-TM-71-1-FBR, Air Force Flight Dynamics Laboratory, 1971.
12. Chang, J.B., Hiyama, R.M., and Szamossi, M., "Improved Methods for Predicting Spectrum Loading Effects, Volume I - Technical Summary," Technical Report AFWAL-TR-81-3092, Air Force Flight Dynamics Laboratory, November 1981.